Validation of *PLAXIS MoDeTo* based on the Cowden till PISA field tests

Eleni Minga and Harvey Burd
Oxford University, UK
6/2/2019

1. Introduction

This document describes a validation example for the PISA methodology implemented in *PLAXIS MoDeTo* (Panagoulias *et al.* 2018) for a clay soil, based on the results obtained from the pile tests conducted at Cowden during the PISA project.

During the PISA project, data from the Cowden pile tests were used to develop and validate the 1D PISA design model as follows:

(a) A ground profile and constitutive model calibration was developed for the Cowden test site based on the available site investigation data (Zdravković *et al.* 2019a). 3D finite element models, based on these data, were then used to analyse the response of the test piles at Cowden (Zdravković *et al.* 2019b). Comparisons between the measured response of the test piles and the corresponding finite element results confirmed the validity of the calibration data and the 3D finite element modelling procedures.

(b) A separate ground model was developed, for a 'representative glacial till offshore site'. This model was closely-based on the conditions at the Cowden site, but with certain modifications (e.g. to the initial pore pressure distribution) to ensure that the ground model is representative of conditions at a submerged offshore site (noting that the Cowden site is onshore). 3D finite element calibration calculations, using the constitutive model calibration data from Step (a), together with the representative glacial till offshore site ground profile, were then used to determine the PISA 1D model parameters for this particular representative offshore site.

In the current document, an alternative process is adopted to demonstrate a validation of the *PLAXIS MoDeTo* model as follows:

(c) Develop a ground profile and constitutive model calibration for the Cowden test site using the NGI-ADP model (Andersen & Jostad 1999).

(d) Conduct a calibration exercise for the *PLAXIS MoDeTo* approach, using the calibration for the Cowden site from Step (c). The calibration pile set consists of pile geometries that straddle the geometric parameters of one of the medium diameter Cowden test piles (CM9, $D = 0.762\mathrm{m}, L = 3.98\mathrm{m}$) .

(e) Demonstrate that the calibrated *PLAXIS MoDeTo* model provides a close fit with the measured response of CM9.

It should be noted that in these calibration calculations the site is onshore. Any gap that forms between the soil and the pile as it is loaded is assumed not to fill with water; as a consequence, the unit weight adopted for the soil is the *saturated bulk unit weight*. This contrasts with an offshore site, where any gaps at the soil-pile interface will immediately fill with water; in this case, the *submerged unit weight* should be adopted for the soil. The modelling procedures described in the current document (employing the saturated bulk unit weight) therefore differ from the procedures that would be normally be employed in practice (based on the submerged unit weight).

A further consideration is that the soil shear strength variation at the Cowden site has a very significant nonlinear variation with depth in the top 5m. Since the calibration piles all lie in this surface region, the performance of the *MoDeTo* calibration process is likely to be slightly less accurate than in practical design cases in which the piles are typically significantly longer than the length scale of any spatial variations with depth in the soil strength profile.

The first part of this document describes the calibration of the NGI-ADP model for the Cowden till soil profile. This calibration is based on (i) site investigation data obtained before the PISA field tests and (ii) subsequent triaxial compression (TXC) tests performed by Imperial College during the PISA project. This ground model calibration is demonstrated by analysing, using PLAXIS 3D (Brinkgreve *et al.* 2018), three of the Cowden test piles and comparing the computed results with the field test data. The document then describes the calibration of a *PLAXIS MoDeTo* 1D model for the Cowden site.

2. Calibration of the NGI-ADP model

A 3D finite element model of the test monopiles at the Cowden site has been developed using the NGI-ADP soil constitutive model as described below. The NGI-ADP model employs the parameters in Table 1.

Table 1. Material parameters for the NGI-ADP model

Parameter	Description
γ_{sat} (kN/m^3)	Saturated unit weight
K_0^{total}	Lateral earth pressure coefficient for total stresses
s_u^A (kPa)	Undrained shear strength with linear distribution within a given soil layer
$s_{u,inc}^A$ (kPa/m)	
G_{ur}/s_u^A	Shear modulus ratio (where G_{ur} is interpreted as having the same meaning as the small strain shear modulus G_o)
s_u^C/s_u^A	Ratio between undrained shear strength for triaxial compression (TXC) and s_u^A
s_u^P/s_u^A	Ratio between undrained shear strength for triaxial extension (TXE) and s_u^A
s_u^{DSS}/s_u^A	Ratio between undrained shear strength for direct simple shear (DSS) and s_u^A
τ_0/s_u^A	
$\gamma_f{}^C$ (%)	Ultimate plastic strain for compression
$\gamma_f{}^E$ (%)	Ultimate plastic strain for extension
$\gamma_f{}^{DSS}$ (%)	Ultimate plastic strain for direct shear

The saturated unit weight of Cowden till has been estimated at $\gamma_{sat} = 21.19\ kN/m^3$ (Zdravković et al. 2019a).

Profiles of the undrained shear strength, s_u^C for triaxial compression (TXC), small strain shear modulus, G_0, and the lateral earth pressure coefficient in terms of effective stresses, K_0, at Cowden were established during the PISA project (Zdravković et al. 2019a). These profiles are shown in Fig. 1. This ground model was used, directly, to determine the values of s_u^C, G_{ur} (assumed to be equivalent to G_o) and K_0^{total} (i.e. the value of K_0 for the total stresses) for the NGI-ADP soil model. [Note that Fig. 1 provides data on the value of K_0 for the *effective* stresses. Values of K_0^{total} for use in the NGI-ADP model are determined from these data using Equations 1-5]. The NGI-ADP model adopts a linear depth

variation of s_u^c and G_{ur}, and a constant value of K_0^{total} in each soil layer. To obtain a reasonable representation, a relatively large number of layers (12 layers in the top 22m of the soil profile) is adopted in the model. Soil layers of thickness 1m were employed to a depth of 6m, to provide an appropriate model for the significant variation of undrained shear strength close to the surface. At greater depths, thicker layers are employed. The piecewise-linear profiles adopted in the PLAXIS 3D ground model are indicated as 'PLAXIS' in Fig. 1.

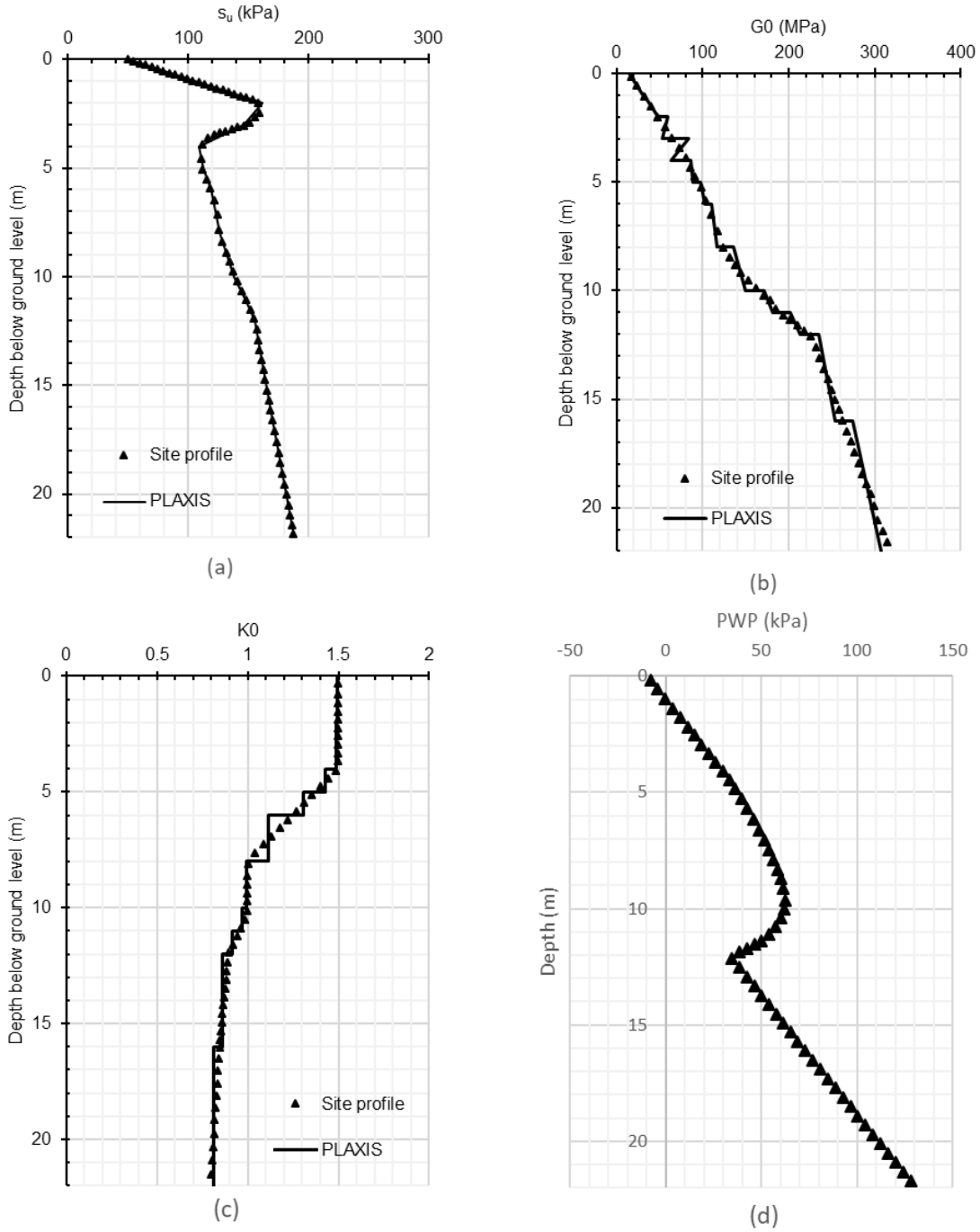

Figure 1. Cowden till ground model (a) triaxial compression (TXC) undrained shear strength (b) small strain shear modulus, G_o (c) lateral earth pressure coefficient (in terms of effective stress) K_o; (d) pore water pressure, u. Cowden site data from (Zdravković et al. 2019a,b).

The ratio s_u^C/s_u^A is set to the default value 0.99. The s_u^A profile can therefore be determined directly from the s_u^C profile in Fig. 1(a). It is noted that the negative gradient of s_u^C (and therefore s_u^A) in the layers between depths of 2m and 4m causes a negative gradient of the simulated G_o (due to the constant ratio G_{ur}/s_u^A in the layer). The thickness of these layers is small, however, and so the influence of these locally-unrealistic G_o gradients is unlikely to be significant.

The K_0 profile in Fig. 1(c) corresponds to the effective stresses. Since NGI-ADP is a total stress model, and the calculations in this case are based on the bulk unit weight γ_{sat}, the K_0^{total} profile needs to be determined. Values of K_0^{total} at the mid-depth of each layer were calculated as follows:

$$\sigma_v = z\,\gamma_{sat} \tag{1}$$

where *z* is distance beneath the ground surface.

$$\sigma_v' = \sigma_v - u \tag{2}$$

where *u* is pore pressure determined at the appropriate depth from the data in Fig. 1(d).

$$\sigma_h' = K_0\sigma_v' \tag{3}$$

where K_0 is determined from the data in Fig 1(c)

$$\sigma_h = \sigma_h' + u \tag{4}$$

$$K_0^{total} = \sigma_h/\sigma_v \tag{5}$$

The triaxial tests performed during the PISA project indicated that the average ultimate stress ratios *q*/*p*′ in triaxial compression (TXC) and triaxial extension (TXE) are 1.07 and 0.9 respectively (Zdravković et al. 2019a).

Therefore,

$$s_u^p/s_u^C = 0.90/1.07 = 0.841 \tag{6}$$

This gives,

$$s_u^P/s_u^A = (s_u^P/s_u^C)(s_u^C/s_u^A) = 0.841 \times 0.99 = 0.833 \tag{7}$$

The undrained shear strength for direct simple shear s_u^{DSS} is taken as the average of s_u^p and s_u^c. This gives,

$$s_u^{DSS}/s_u^A = \frac{1}{2}(s_u^C + s_u^P)/s_u^A = 0.911 \tag{8}$$

The value of τ_0/s_u^A in each layer is determined from,

$$\frac{\tau_0}{s_u^A} = -0.5(1-K_0)\frac{\sigma_{v,0}'}{s_u^A} = -0.5\left(1-K_0^{total}\right)\frac{\sigma_{v,0}}{s_u^A} \tag{9}$$

When the value calculated by Equation (9) is negative, the τ_0/s_u^A ratio is set to zero. In the current example, the soil has relatively high values of K_0 near the surface; the value of τ_0/s_u^A determined on this basis is either zero or, for depths greater than about 10m, a small positive value. Separate numerical experiments were conducted with τ_0/s_u^A=0.7 for all of the layers, but the resulting PLAXIS 3D models of the Cowden field test piles were all unrealistically stiff.

Table 2. Specifications of the initial conditions for the Cowden TXC triaxial tests (Zdravković et al. 2019a).

Depth (m)	K_0	σ_v' (kPa)	σ_h' (kPa)	*u* (kPa)	σ_v (kPa)	σ_h (kPa)	K_0^{total}
2.5	1.5	41.1	61.7	14.6	55.7	76.2	1.368
5	1.5	69.5	104.3	37.7	107.2	142.0	1.325
8.2	1.0	121.0	121.0	58.1	179.1	179.1	1.000

The values of the parameters γ_f^C, γ_f^E and γ_f^{DSS} were based on the results of TXC tests on Cowden till samples taken from depths of 2.5m, 5m and 8.2m. These TXC tests, conducted by Imperial College during the PISA project, are specified in Table 2. The effective stress conditions indicated Table 2 – which are the stresses actually applied during the initial K_o consolidation stage - relate approximately to the estimated *in situ* stresses for each sample depth. The pore pressures, *u*, in Table 2 (required to determine the appropriate total stresses to facilitate the NGI-ADP analysis of the tests) have been determined from the pore pressure profile in Fig.1(d).

The triaxial tests were simulated in PLAXIS 3D (using a finite element model for the test rather than the soil test facility). Calculations were conducted in two stages. Initially the sample was compressed by applying the total stresses indicated in Table 2. Then, in the second stage, axial compression was applied. During the calibration, the ratios between the three plastic strain parameters were kept constant at $\gamma_f^E = 2\gamma_f^C$ and $\gamma_f^{DSS} = 1.5\gamma_f^C$. It was considered that γ_f^C varies as a function of the ratio G_{ur}/s_u^A, based on the equation (Panagoulias *et al.* 2018),

$$\gamma_f^C = K_f \cdot 100/(\frac{G_{ur}}{s_u^A}) \tag{10}$$

where K_f is the single calibration parameter that is adjusted to provide, by eye, the best fit between the TXC results and the PLAXIS 3D results. The calibration data for the model obtained from this process are listed in Table 3.

Table 3. Calibration of the NGI-ADP model for Cowden till. [Note that the water table is taken to be at 1m below the ground surface.]

Layer	Depth (m)	K_0	u (kPa)	K_0^{total}	s_u^A (kPa)	$s_u^A{}_{inc}$ (kPa/m)	γ_{sat} (kN/m³)	G_{ur}'/s_u^A	s_u^P/s_u^A	s_u^{DSS}/s_u^A	τ_0/s_u^A	K_f	$\gamma_f{}^C$ (%)	$\gamma_f{}^E$ (%)	$\gamma_f{}^{DSS}$ (%)
1	0	1.500	-4.950	1.500	50.149	56.626	21.19	289.107	0.833	0.911	0.000	190	65.720	131.439	98.580
	1				106.775										
2	1	1.500	4.929	1.422	106.775	56.626	21.19	290.504	0.833	0.911	0.000	150	51.634	103.269	77.452
	2				163.401										
3	2	1.500	14.571	1.362	163.401	-15.298	21.19	361.861	0.833	0.911	0.000	120	33.162	66.324	49.743
	3				148.103										
4	3	1.500	23.999	1.338	148.103	-37.555	21.19	568.968	0.833	0.911	0.000	120	21.091	42.182	31.636
	4				110.548										
5	4	1.500	33.237	1.283	110.548	3.263	21.19	784.927	0.833	0.911	0.000	120	15.288	30.576	22.932
	5				113.811										
6	5	1.305	41.274	1.197	113.811	6.736	21.19	854.320	0.833	0.911	0.000	120	14.046	28.093	21.069
	6				120.547										
7	6	1.117	51.200	1.077	120.547	3.711	21.19	916.135	0.833	0.911	0.000	120	13.099	26.197	19.648
	8				127.969										
8	8	0.992	60.110	0.994	127.969	6.056	21.19	1065.790	0.833	0.911	0.003	120	11.259	22.519	16.889
	10				140.081										
9	10	0.970	60.066	0.978	140.081	8.624	21.19	1224.000	0.833	0.911	0.013	120	4.902	9.804	7.353
	11				148.704										
10	11	0.918	45.797	0.934	148.704	8.322	21.19	1355.089	0.833	0.911	0.038	120	4.428	8.856	6.642
	12				157.026										
11	12	0.863	52.864	0.888	157.026	3.243	21.19	1492.755	0.833	0.911	0.071	120	4.019	8.039	6.029
	16				169.998										
12	16	0.816	101.182	0.862	169.998	3.379	21.19	1613.928	0.833	0.911	0.116	120	3.718	7.435	5.576
	22				190.275										

Figure 2 shows the comparison between the experimental TXC data and the corresponding PLAXIS 3D simulations employing the calibrated model. A generally good agreement is obtained. The results of the simulated TXC tests have been used to determine the degradation of the secant shear modulus with incremental deviatoric strain, $\delta\varepsilon_d$, where the general form of incremental deviatoric strain (in terms of principal stresses) is (Potts and Zdravković 2001):

$$\delta\varepsilon_d = \sqrt{\frac{2}{3}[(\delta\varepsilon_2 - \delta\varepsilon_3)^2 + (\delta\varepsilon_1 - \delta\varepsilon_2)^2 + +(\delta\varepsilon_1 - \delta\varepsilon_3)^2]} \tag{11}$$

For undrained triaxial compression conditions, this reduces to,

$$\delta\varepsilon_d = \sqrt{3}\,\delta\varepsilon_a \tag{12}$$

where $\delta\varepsilon_a$ is the incremental axial strain.

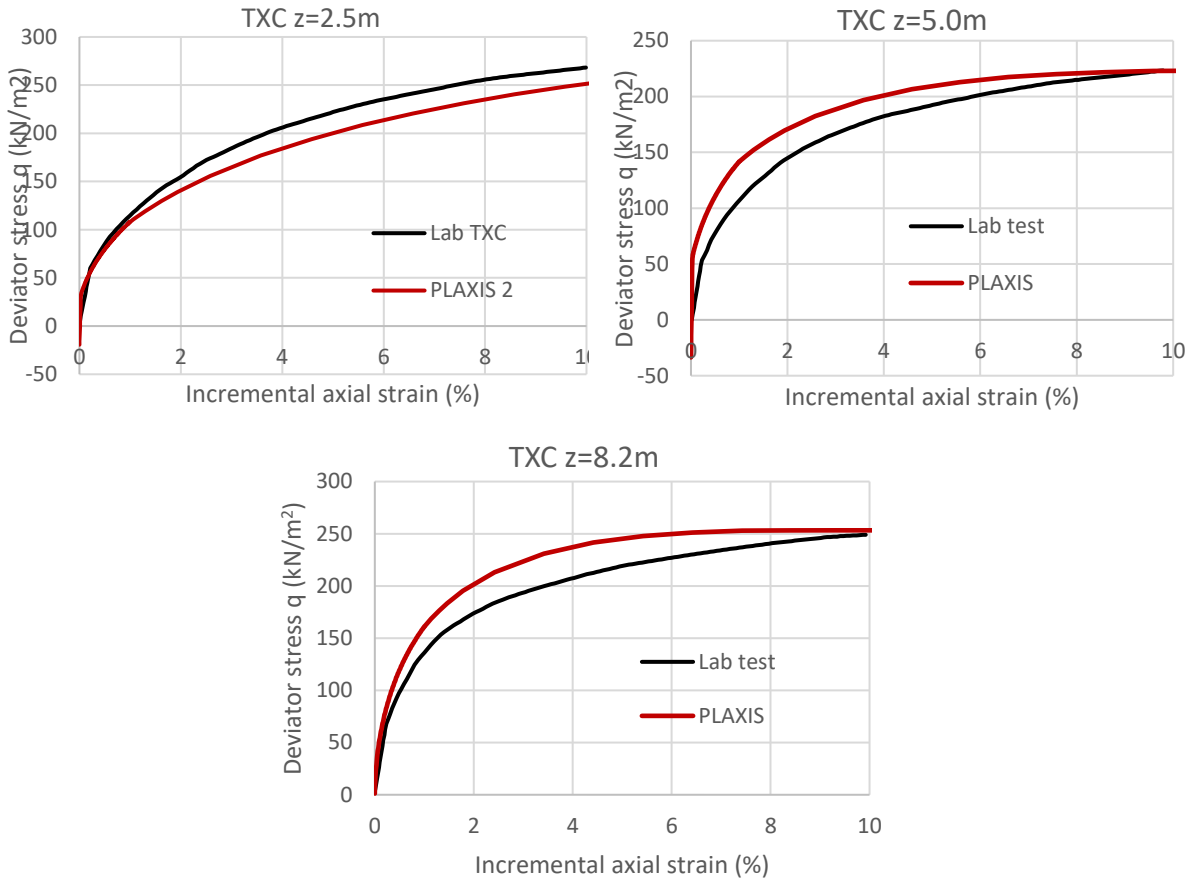

Figure 2. TXC tests; comparison of experimental result and PLAXIS 3D simulations using the NGI-ADP model. Triaxial test data from (Zdravković et al. 2019b).

The secant shear modulus degradation data are plotted in Fig. 3 (noting that the deviatoric strain in these plots refers to incremental deviatoric strain with reference to the sample state at the end of the K_0^{total} compression stage). These data are compared in Fig. 3 with the secant shear modulus degradation adopted in the ICFEP model that was employed during PISA to model the Cowden test piles. The equation of this nonlinear stiffness degradation model (in terms of the tangent shear modulus) is given as Equation 4 of Zdravković et al. 2019b as,

$$G_{tan} = 1100p' \left(0.05 + \frac{0.095}{1 + \left({\delta\varepsilon_d}/{9.78 \times 10^{-5}} \right)^{0.987}} \right) \tag{13}$$

The comparisons in Fig 3 indicate that, for the 2.5m and 5m deep samples, the maximum shear strain (G_o or G_{ur}) plateau extends to larger strains than is implied by the PISA model (implemented in ICFEP). This is due to the influence of the relatively high value of K_0^{total} in these two samples. At the start of the axial compression stage, the axial stress is the minor principal stress; relatively large axial strains are therefore required to mobilise the yield surface for the case where the axial stress becomes the major principal stress. This influence of K_0^{total} is not present in the nonlinear elastic model used in the

ICFEP model. This extended plateau does not occur in the PLAXIS model for the 8.2m deep sample because, in this case, the axial compression stage begins with a K_0^{total} of 1.0.

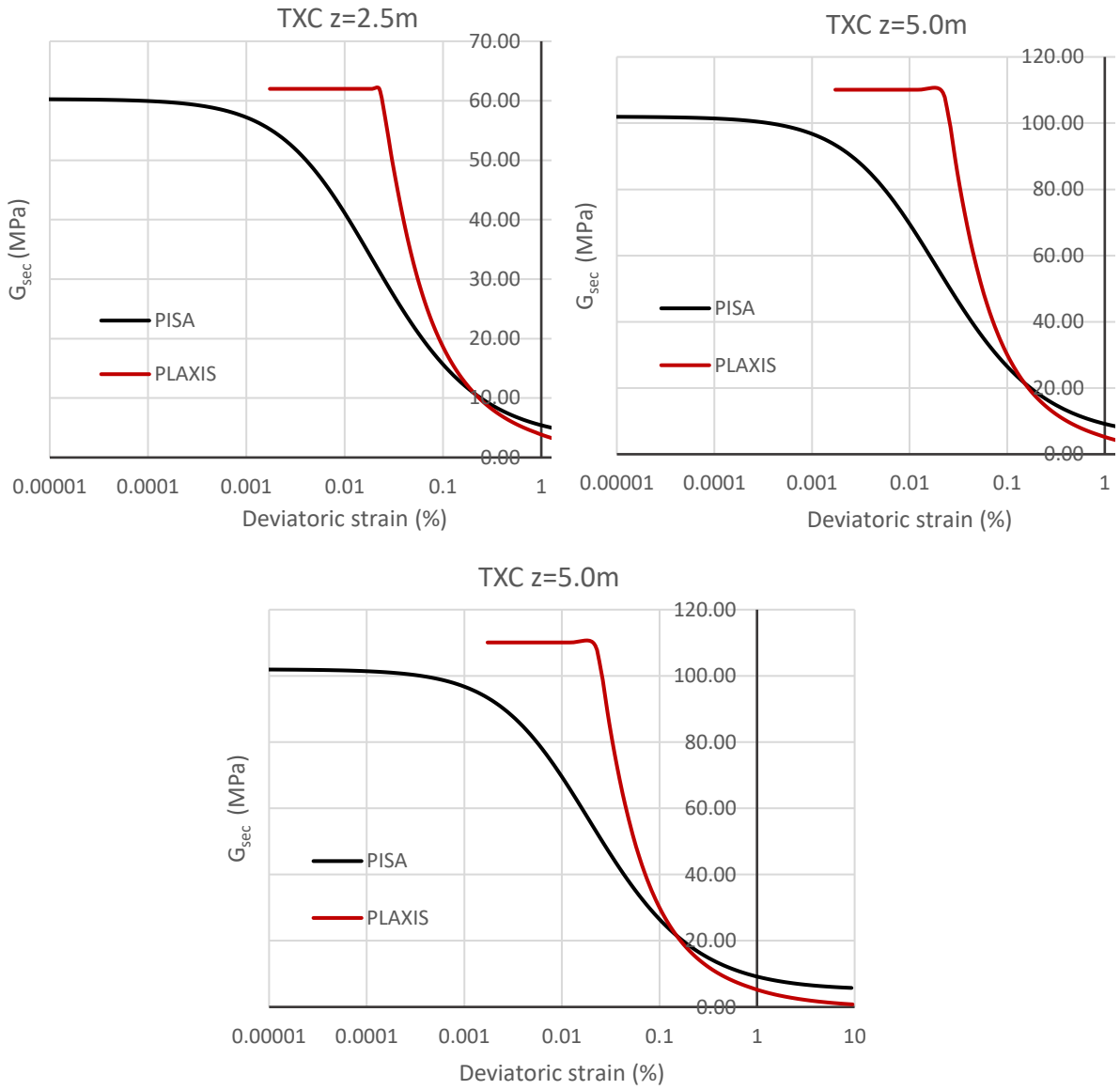

Figure 3. Degradation of secant shear modulus, G_{sec}. (The data labelled 'PISA' refer to the assumed non-linear elastic model employed in the PISA ICFEP 3D finite element calculations, Zdravković et al. 2019b)

3. Analysis of the PISA test piles

Three of the Cowden field tests have been simulated using PLAXIS 3D, employing the parameters listed in Table 4. The calculation type chosen for the soil layers was Undrained C. Interface elements, with Mohr-Coulomb behaviour, are placed between the soil and the pile. The stiffness parameters of the interfaces are similar to the stiffness of the adjacent soil layers, while the strength is reduced by a factor of 0.65 (Panagoulias *et al.* 2018). The calculation type for the interface elements is Drained.

The geometry of the analysed piles is specified in Fig. 4 and Table 4. Comparisons between the PLAXIS 3D results and the field test data are shown in Figs. 5-7.

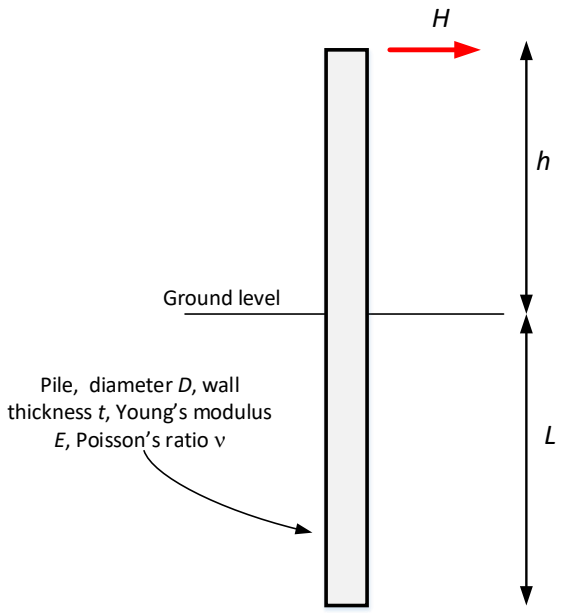

Figure 4. Geometric parameters of for the test piles

Table 4. Geometric characteristics of piles tested in Cowden and simulated in PLAXIS 3D (from Byrne et al. 2019)

Pile	D (m)	L (m)	t (m)	h (m)
CM2	0.762	2.24	0.010	10.06
CM9	0.762	3.98	0.011	9.98
CL1	2.000	10.35	0.025	10.10

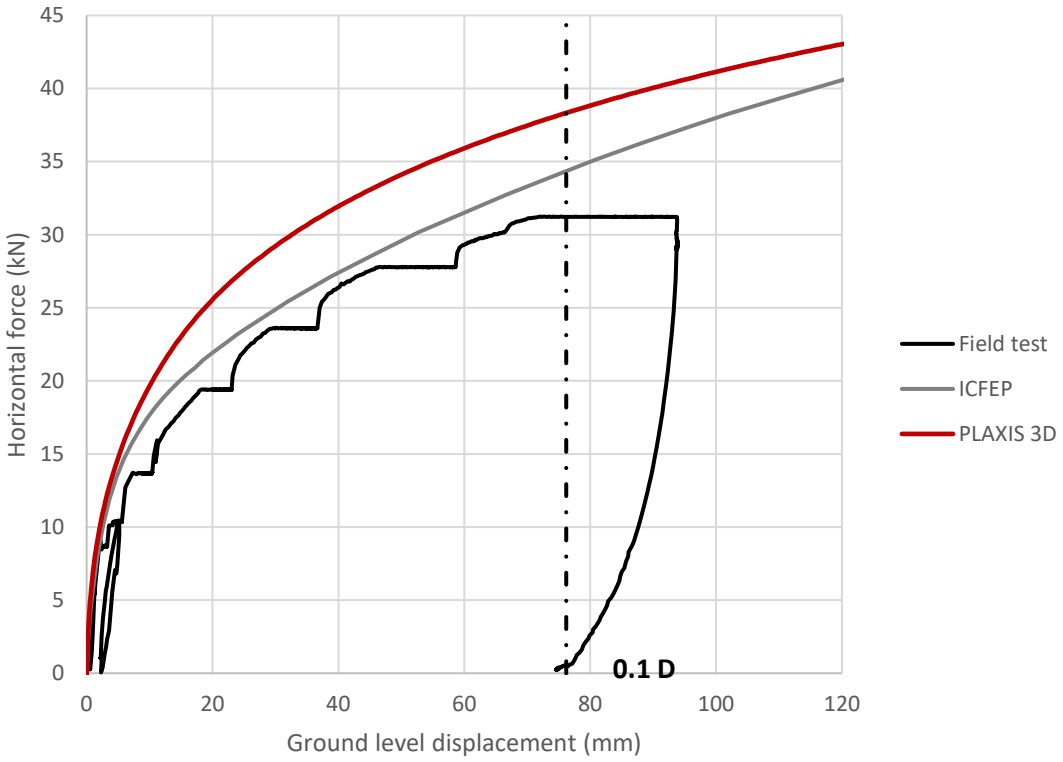

Figure 5. Pile CM2 (D=0.762m, L=2.24m): Comparison between the field data and PLAXIS 3D results. (Field test data from Byrne et al. 2019; ICFEP data from Zdravković et al. 2019b)

The PLAXIS 3D simulations (Figs. 5-7) provide reasonable representations (similar in quality to the ICFEP calculations developed during the PISA project) of the observed response of the test piles up to the assumed ultimate limit state pile ground level displacement of $v_G = 0.1D$. The numerical response of the (shorter) pile CM2 is stiffer than the field test data (Fig. 5), suggesting that the soil model adopted for the superficial layers may not be optimal. However, the response of piles CM9 and CL1, which extend to deeper layers, is accurately reproduced.

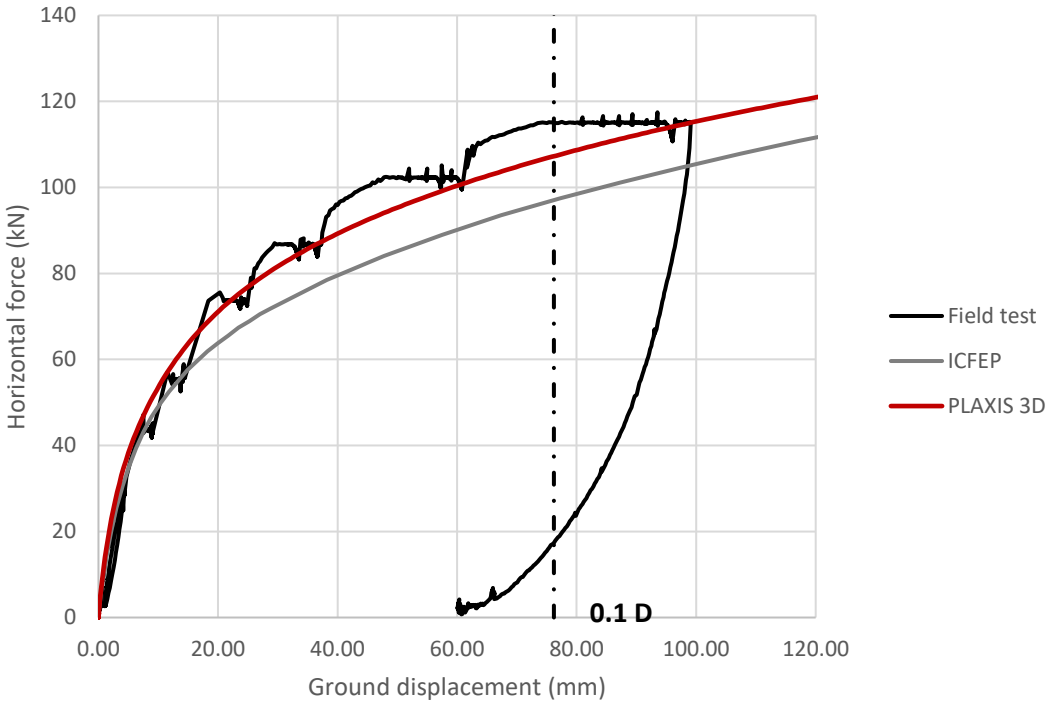

Figure 6. Pile CM9 (D=0.762m, L=3.98m): Comparison between the field data and PLAXIS 3D results. Field test data from Byrne et al. 2019; ICFEP data from Zdravković et al. 2019b

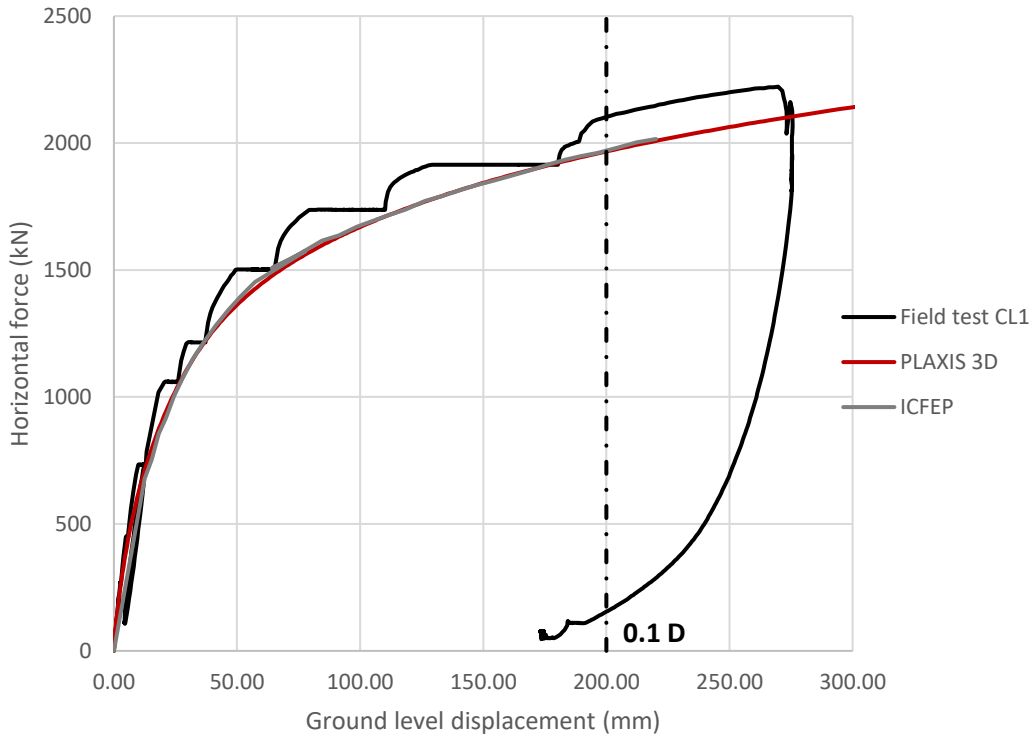

Figure 7. Pile CL1 (D=2m, L=10.35m): Comparison between the field data and PLAXIS 3D results. Field data from Byrne et al. 2019; ICFEP results from Zdravković et al. 2019b

4. Calibration of the *PLAXIS MoDeTo* 1D model

A calibrated *PLAXIS MoDeTo* 1D model (based on the latest version, incorporating the second stage optimisation) for the Cowden site has been developed. This calibrated *PLAXIS MoDeTo* 1D model has then been used to simulate the response of pile CM9 (D=0.762m, L/D=5.2).

The soil properties given as input in *PLAXIS MoDeTo* for the calibration of the 1D model, based on the data in Table 3) are provided in Table 5. The *PLAXIS MoDeTo* 1D model is calibrated using the 'calibration set' specified Table 6. The selected parameter space spans the parameters for pile CM9 (although this particular pile geometry is not included in the calibration set). The models GeoDS_1 – GeoDs_8 are generated automatically in *PLAXIS MoDeTo*.

Table 5. Soil profile defined in PLAXIS MoDeTo

Layer	Top (m)	Bottom (m)	Saturated unit weight (kN/m^3)	G_0 (kN/m^2)	$s_{u,top}$ (kN/m^2)	$s_{u,bottom}$ (kN/m^2)	K_0^{total}
1	0.000	-1.000	21.19	22684	50.15	106.8	1.500
2	-1.000	-2.000	21.19	39243	106.8	163.8	1.422
3	-2.000	-3.000	21.19	56361	163.8	148.1	1.362
4	-3.000	-4.000	21.19	73582	148.1	110.5	1.338
5	-4.000	-5.000	21.19	88053	110.5	113.8	1.283
6	-5.000	-6.000	21.19	100108	113.8	120.5	1.197
7	-6.000	-8.000	21.19	113837	120.5	128.0	1.077
8	-8.000	-10.000	21.19	142842	128.0	140.1	0.994

Table 6. Calibration set

Reference	D (m)	h(m)	L/D	L (m)	t (mm)	D/t	h/L
GeoDS_1	0.65	5	4.5	2.925	11	59.09	1.71
GeoDS_2	0.65	5	5.5	3.575	11	59.09	1.40
GeoDS_3	0.85	5	4.5	3.825	11	77.27	1.31
GeoDS_4	0.85	5	5.5	4.675	11	77.27	1.07
GeoDS_5	0.85	15	4.5	3.825	11	77.27	3.92
GeoDS_6	0.85	15	5.5	4.675	11	77.27	3.21
GeoDS_7	0.65	15	4.5	2.925	11	59.09	5.13
GeoDS_8	0.65	15	5.5	3.575	11	59.09	4.20

A PLAXIS 3D model for each of the calibration piles was generated and calculated in *PLAXIS MoDeTo*. Each pile was subjected to a lateral force *H* that was sufficient for the pile ground level displacement, v_G, to reach a value of between $2.3 \times D/10$ and $2.8 \times D/10$. This magnitude of displacement is necessary for reliable determination of the ultimate resistance parameters for the 1D model. The parameterisation procedure was then launched and the depth variation functions for the soil reactions were computed.

The accuracy of the calibrated 1D model was initially checked by comparison with the calibration set. Plots showing the $H - v_G$ responses from the PLAXIS 3D model and the *PLAXIS MoDeTo* 1D model for each of the calibration piles are shown in Figs. 9 and 10. The plots in the left column correspond to v_G in the range 0 to *D*/10,000 (referred to as the 'small displacement' range); the plots in the right column show the computed response for v_G in the range 0 to *D*/10 (referred to as the 'large

displacement' range). The accuracy of the 1D model is quantified using an 'accuracy metric' which is defined,

$$\eta = \frac{A_{ref} - A_{diff}}{A_{ref}} \tag{14}$$

where the meaning of A_{ref} and A_{diff} are illustrated in Fig. 8.

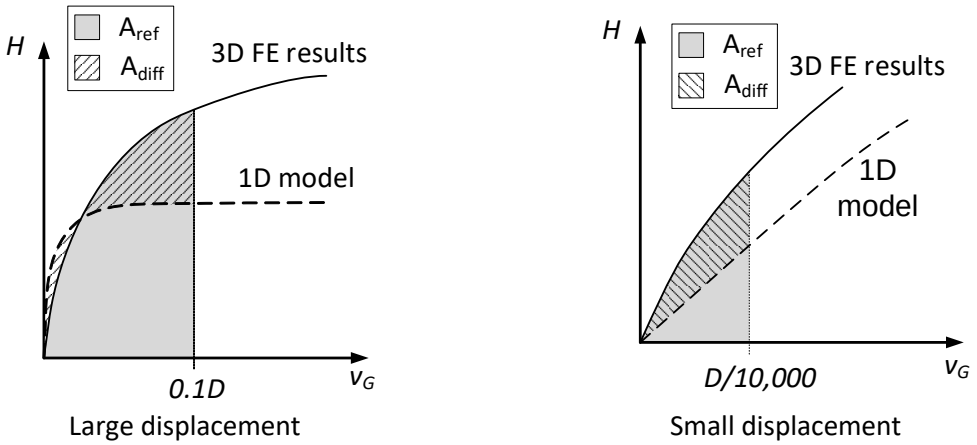

Figure 8: Accuracy metric

The accuracy metric η was calculated for each pile for both displacement ranges; these values are listed in Table 7. The quality of fit metric is greater than 0.9, except for four small displacement cases, in indicating a successful calibration.

Although a reasonable match between the 1D model and the 3D calibration data is obtained, a key aspect of this particular ground model needs to be noted. The profile of undrained shear strength in the top 5m of the soil at the Cowden site is highly variable with depth. The length of the piles in the calibration set all lie in this highly non-uniform soil. As a consequence, the general shape of the strength profile relevant to pile GeoDS_1 (length 2.25 m, shear strength increasing approximately linearly with distance along the pile) is significantly different than, for example, pile GeoDS_8 (length 5.5m with a positive followed by a negative shear strength gradient along the pile). Calibrating the 1D model over a significant range of shear strength profile 'shapes' presents a significant challenge for the optimisation procedures in the 1D model. For current wind turbine applications, piles tend to be of lengths between about 20m and 50m. In these cases (which are consistent with the calibration space considered in the PISA project) the influence of any non-uniform surface layers is likely to be less significant.

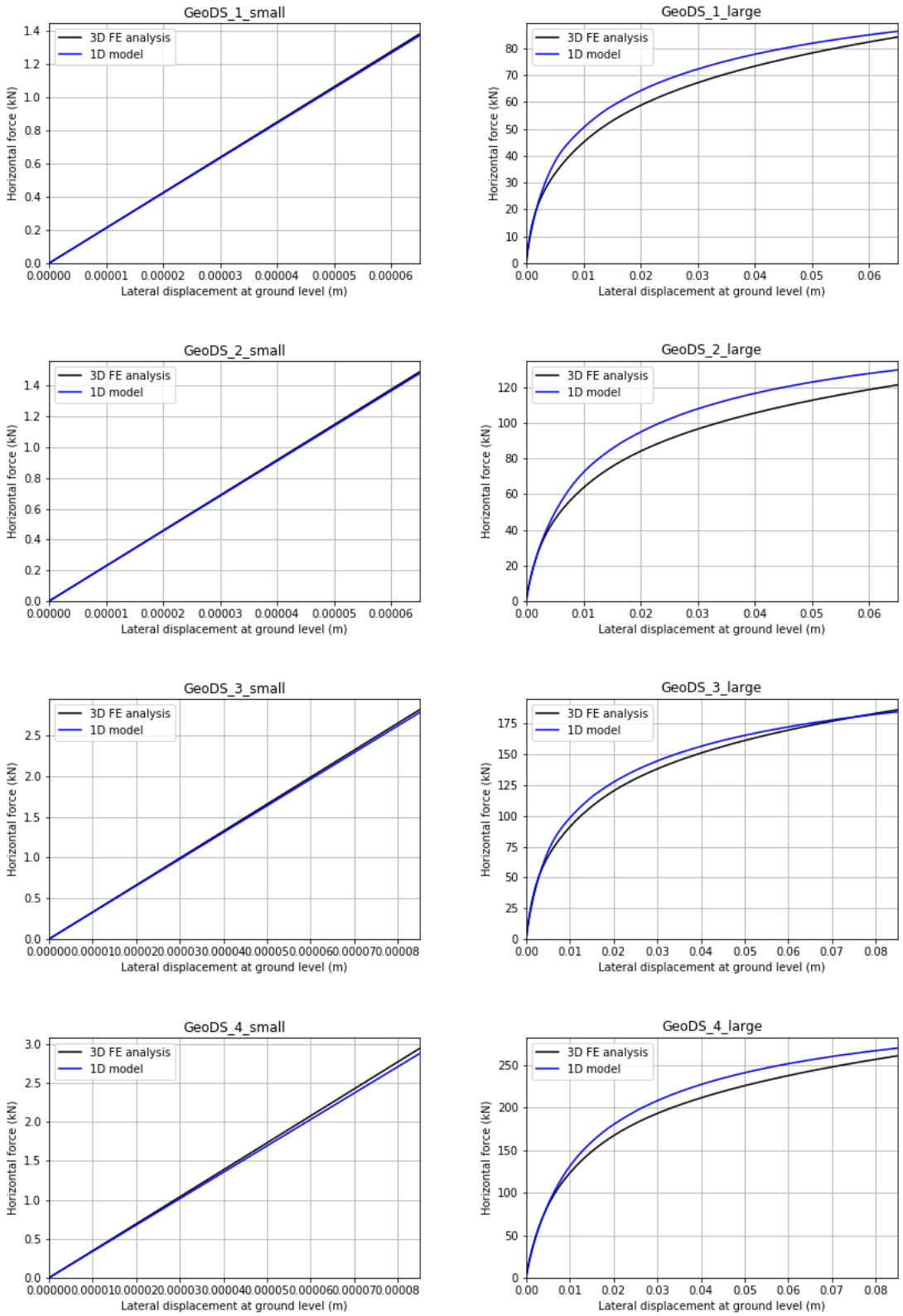

Figure 9. Comparison between the response of the PLAXIS 3D model and the response of the calibrated 1D model for piles GeoDS_1 to GeoDS_4

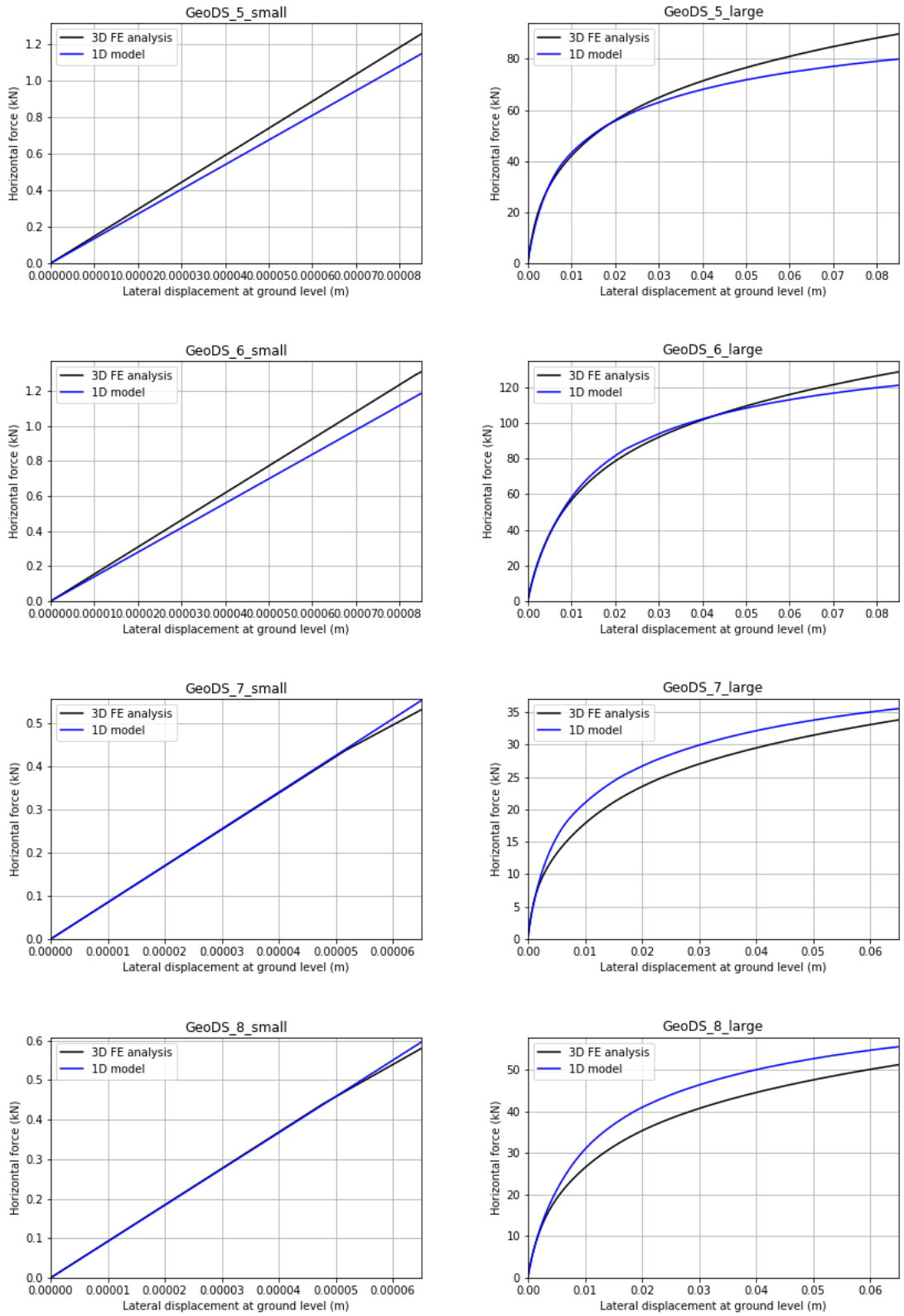

Figure 10. Comparison between the response of the PLAXIS 3D model and the response of the calibrated 1D model for piles GeoDS_5 to GeoDS_8

Table 7. Accuracy metric for the calibration piles in the small and large displacement ranges

Pile	η small	η large
GeoDS_1	0.993	0.934
GeoDS_2	0.993	0.897
GeoDS_3	0.988	0.971
GeoDS_4	0.978	0.939
GeoDS_5	0.913	0.939
GeoDS_6	0.906	0.972
GeoDS_7	0.960	0.900
GeoDS_8	0.972	0.877
Mean	**0.963**	**0.929**

5. Response prediction for pile CM9

Figure 11 shows the $H - v_G$ response for CM9 computed with the calibrated *PLAXIS MoDeTo* 1D model. The response is seen to agree well with the PLAXIS 3D analysis for this pile and also the measured field data. The quality of fit metrics for the small and large displacements – derived based on the comparison between the PLAXIS 3D and *PLAXIS MoDeTo* 1D responses – are listed in Table 8.

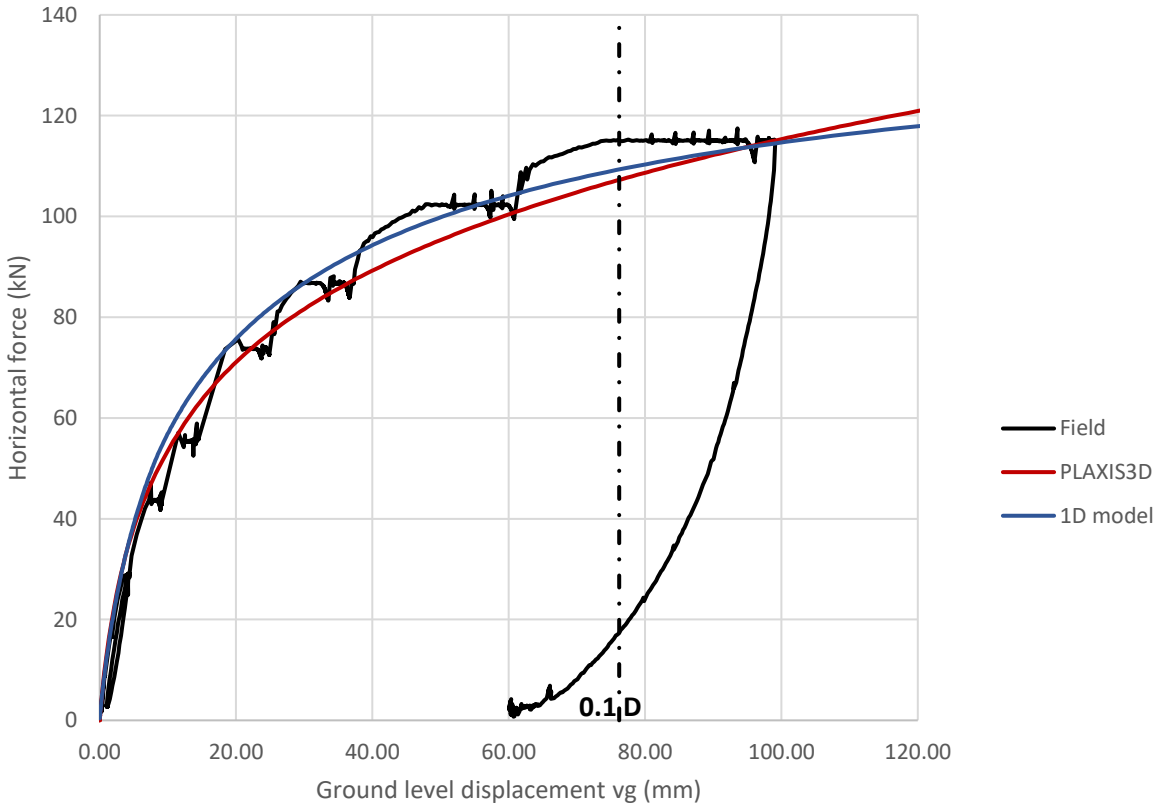

Figure 11. Response of 1D model of Pile CM9 compared to the field rest results and the PLAXIS 3D data. Field test data from Byrne et al. 2019

Table 8. Accuracy metrics for pile CM9 in the small and large displacement range

Pile	η small	η large
CM9	0.906	0.953

6. Conclusions

This document describes an application of the *PLAXIS MoDeTo* system to the analysis of the PISA test monopiles at the Cowden test site. Initially, a calibration for the NGI-ADP model is developed, based on geotechnical data collected during the PISA project. PLAXIS 3D is then employed, using the calibrated NGI-ADP model, to analyses the monotonic loading performance of three of the PISA test piles; the close comparison between the field test data and the PLAXIS 3D results confirms the validity of the NGI-ADP model calibration.

A separate exercise is then conducted in which the *PLAXIS MoDeTo* is calibrated using a set of eight calibration piles, based on the soil conditions at the Cowden site but not including the dimensions of the piles that were actually tested. The calibrated model is then used to predict one of the PISA test piles; the close fit between the *PLAXIS MoDeTo* response and the field data (accuracy metric values greater than 0.9) demonstrates the effectiveness of the *PLAXIS MoDeTo* calibration process.

The analyses described above relate to an onshore site. For practical offshore design applications, however, the site will be submerged. In these cases, to provide a correct representation of the influence of any gap that forms between the pile and the ground, the submerged using weight should be employed for the soil (rather than the bulk unit weight as employed in the calculations described in this document).

References

Andersen, L., Jostad, H.P. (1999). Application of an anisotropic hardening model for undrained response of saturated clay. In Proc. Numerical Models in Geomechanics - NUMOG VII, Graz, Austria.

Brinkgreve, R.B.J., Kumarswamy, S. and Swolfs, W.M. (2018). PLAXIS manual 2018. Plaxis bv, Delft, the Netherlands.

Byrne, B.W., McAdam, R.A., Burd, H.J., Beuckealers, W.J.A.P., Gavin, K., Houlsby, G.T., Igoe, D., Jardine, R.J., Martin, C.M., Muir Wood, A., Potts, D.M., Skov Gretlund, J., Taborda, D.M.G. and Zdravković, L. (2019) Monotonic laterally loaded pile testing in a stiff glacial clay till at Cowden *Géotechnique* (in press).

Panagoulias, S., Brinkgreve, R.B.J., Zampich, L. (2018). PLAXIS MoDeTo manual 2018. Plaxis bv, Delft, the Netherlands.

Potts, D. M., & Zdravković, L. (2001). Finite element analysis in geotechnical engineering: application (Vol. 2). Thomas Telford.

Zdravković, L., Jardine, R.J., Taborda, D.M.G., Abadias, D., Burd, H.J., Byrne, B.W., Gavin, K., Houlsby, G.T., Igoe, D., Liu, T., Martin, C.M., McAdam, R.A., Muir Wood, A., Potts, D.M., Skov Gretlund, J. and Ushev, E. (2019a) Ground characterisation for PISA pile testing and analysis *Géotechnique* (in press).

Zdravković, L, Taborda, D.M.G., Potts, D.M., Abadias, D., Burd, H.J., Byrne, B.W., Gavin, K., Houlsby, G.T., Jardine, R.J., Martin, C.M., McAdam, R.A., Emil Ushev, E. (2019b) Finite element modelling of laterally loaded piles in a stiff glacial clay till at Cowden. *Géotechnique* (in press).